2018-01-02

HIV-1 R5 Macrophage-Tropic Envelope Glycoprotein Trimers Bind CD4 with High Affinity, while the CD4 Binding Site on Non-macrophage-tropic, T-Tropic R5 Envelopes Is Occluded

Briana Quitadamo
University of Massachusetts Medical School

Et al.

AMERICAN SOCIETY FOR MICROBIOLOGY | Journal of Virology®

VIRUS-CELL INTERACTIONS

HIV-1 R5 Macrophage-Tropic Envelope Glycoprotein Trimers Bind CD4 with High Affinity, while the CD4 Binding Site on Non-macrophage-tropic, T-Tropic R5 Envelopes Is Occluded

Briana Quitadamo,[a] Paul J. Peters,[a]* Alexander Repik,[a] Olivia O'Connell,[a] Zhongming Mou,[a] Matthew Koch,[a] Mohan Somasundaran,[a] Robin Brody,[a] Katherine Luzuriaga,[a] Aaron Wallace,[b]* Shixia Wang,[b] Shan Lu,[b] Sean McCauley,[a] Jeremy Luban,[a] Maria Duenas-Decamp,[a] Maria Paz Gonzalez-Perez,[a] Paul R. Clapham[a]

[a]Program in Molecular Medicine, University of Massachusetts Medical School, Biotech 2, Worcester, Massachusetts, USA

[b]Department of Medicine, University of Massachusetts Medical School, Worcester, Massachusetts, USA

ABSTRACT HIV-1 R5 variants exploit CCR5 as a coreceptor to infect both T cells and macrophages. R5 viruses that are transmitted or derived from immune tissue and peripheral blood are mainly inefficient at mediating infection of macrophages. In contrast, highly macrophage-tropic (mac-tropic) R5 viruses predominate in brain tissue and can be detected in cerebrospinal fluid but are infrequent in immune tissue or blood even in late disease. These mac-tropic R5 variants carry envelope glycoproteins (Envs) adapted to exploit low levels of CD4 on macrophages to induce infection. However, it is unclear whether this adaptation is conferred by an increased affinity of the Env trimer for CD4 or is mediated by postbinding structural rearrangements in the trimer that enhance the exposure of the coreceptor binding site and facilitate events leading to fusion and virus entry. In this study, we investigated CD4 binding to mac-tropic and non-mac-tropic Env trimers and showed that CD4-IgG binds efficiently to mac-tropic R5 Env trimers, while binding to non-mac-tropic trimers was undetectable. Our data indicated that the CD4 binding site (CD4bs) is highly occluded on Env trimers of non-mac-tropic R5 viruses. Such viruses may therefore infect T cells via viral synapses where Env and CD4 become highly concentrated. This environment will enable high-avidity interactions that overcome extremely low Env-CD4 affinities.

IMPORTANCE HIV R5 variants bind to CD4 and CCR5 receptors on T cells and macrophages to initiate infection. Transmitted HIV variants infect T cells but not macrophages, and these viral strains persist in immune tissue even in late disease. Here we show that the binding site for CD4 present on HIV's envelope protein is occluded on viruses replicating in immune tissue. This occlusion likely prevents antibody binding to this site and neutralization of the virus, but it makes it difficult for virus-CD4 interactions to occur. Such viruses probably pass from T cell to T cell via cell contacts where CD4 is highly concentrated and allows infection via inefficient envelope-CD4 binding. Our data are highly relevant for vaccines that aim to induce antibodies targeting the CD4 binding site on the envelope protein.

KEYWORDS CCR5, CD4, CD4bs, HIV, envelope glycoprotein, macrophage tropism

The HIV-1 envelope glycoprotein (Env) on viral particles is arranged as trimers with three copies of surface gp120 and three of transmembrane gp41. HIV infection of cells requires interactions between Env trimers on virus particles with CD4 and a coreceptor, either CCR5 or CXCR4, on the cell surface. These interactions trigger fusion between viral and cell membranes, initiating virus entry (reviewed in reference 1).

HIV-1 R5 Envs exploit CCR5 as a coreceptor to infect both T cells and macrophages.

Received 23 May 2017 **Accepted** 24 October 2017

Accepted manuscript posted online 8 November 2017

Citation Quitadamo B, Peters PJ, Repik A, O'Connell O, Mou Z, Koch M, Somasundaran M, Brody R, Luzuriaga K, Wallace A, Wang S, Lu S, McCauley S, Luban J, Duenas-Decamp M, Gonzalez-Perez MP, Clapham PR. 2018. HIV-1 R5 macrophage-tropic envelope glycoprotein trimers bind CD4 with high affinity, while the CD4 binding site on non-macrophage-tropic, T-tropic R5 envelopes is occluded. J Virol 92:e00841-17. https://doi.org/10.1128/JVI.00841-17.

Editor Frank Kirchhoff, Ulm University Medical Center

Address correspondence to Paul R. Clapham, paul.clapham@umassmed.edu.

* Present address: Paul J. Peters, Department of Molecular, Cell and Cancer Biology, University of Massachusetts Medical School, Worcester, Massachusetts, USA; Aaron Wallace, MassBiologics, Mattapan, Massachusetts, USA.

R5 Envs derived from immune tissue (e.g., lymph node and spleen) and from peripheral blood are inefficient at mediating infection of macrophages. These Envs have been described as R5, non-macrophage tropic (non-mac tropic) (2, 3), or R5, T-cell tropic (4). In contrast, highly mac-tropic R5 Envs are predominant in brain tissue and detected in cerebrospinal fluid (CSF) (4, 5). Mac-tropic R5 variants have also been detected in semen (3, 6, 7) but are infrequent in immune tissue or blood even in late disease (3).

On virus particles *in vivo*, native and unliganded Env trimers predominantly form a closed conformation with the three gp120s connecting at the apex via the trimer association domain (TAD), which is comprised of the V1V2 and V3 loops (8–14). When CD4 on the cell surface binds an HIV-1 Env spike, it triggers the Env trimer to open and expose a site for binding a coreceptor, usually CCR5 (15). Trimer opening involves the disentanglement of the TAD to enable (i) a shift in the location of the V1V2 loops to expose the V3 loop and (ii) exposure of a determinant on the V1V2 stem that is recruited by CD4 to assemble the bridging sheet. The V3 loop and sections of the bridging sheet form the exposed coreceptor binding site (1). We previously reported that over 50% of highly, mac-tropic Envs carried modified TADs, estimated either by increased V3 loop exposure or by loss of the PG9/16 trimer-specific epitope on V1V2 of the TAD (16). All Envs remained resistant to neutralization by CD4i (CD4-induced) monoclonal antibodies (MAbs) and the CD4 binding site (CD4bs) MAb, b6, indicating that mac-tropic trimers are not wide open but have subtle changes in the TAD that allow CD4 access to the CD4bs or enable the trimer to open more efficiently on encountering CD4. On the native trimer, the configuration of the trimer association domain and glycans that are within it and nearby play an important role in protecting the CD4bs from antibodies (17).

Mac-tropic R5 Envs have adapted to be able to interact efficiently with low CD4 levels to trigger conformational changes in the Env trimer that expose the CCR5 binding site. This enhanced Env-CD4 interaction allows the infection of macrophages, which express substantially smaller amounts of CD4 on their cell surfaces than do T cells (18–20). No specific Env determinant has been identified that universally explains R5 mac tropism. The Gabuzda lab identified N283 (a CD4bs residue) as present in mac-tropic or brain-derived Envs of some subjects that showed enhanced gp120-CD4 interactions (21). However, other determinants have been identified proximal to the CD4bs (22) and within the V1 (23), V2 (24), and V3 (22) loops. It seems likely that any Env determinant that enhances the exposure of the CD4bs will result in an enhanced Env-CD4 interaction and increased macrophage infection. Such determinants may occur in different regions of Env, and it is likely that different determinants in different Envs impact mac tropism. It is also unclear whether the capacity of Env to exploit low CD4 concentrations to trigger entry results from a more efficient initial binding event between Env and CD4, enhanced Env trimer conformational changes in response to CD4 binding, or both. Thus, while several studies have investigated the capacity of R5 mac-tropic and non-mac-tropic viruses to exploit low CD4 to infect cells, none have directly measured or compared CD4 binding to trimeric, native Envs of such variants.

In this study, we investigated CD4 binding to mac-tropic and non-mac-tropic Env trimers expressed on 293T cells. We show that CD4-IgG binds efficiently to mac-tropic R5 Env trimers, while binding to non-mac-tropic trimers was remarkably inefficient or undetectable. This nearly undetectable binding of CD4 to non-mac-tropic Envs presumably reflects an adaptation to protect this site from antibodies but at a cost of compromising Env-CD4 binding. Nevertheless, this observation for non-mac-tropic Env trimers is remarkable considering that all HIV-1 variants must bind CD4 to gain entry into cells. Our data may therefore point toward a preferred route of entry into T cells for non-mac-tropic R5 viruses across viral synapses where Env and CD4 become highly concentrated (25, 26) and thus enable high-avidity interactions that can overcome extremely low Env-CD4 affinities.

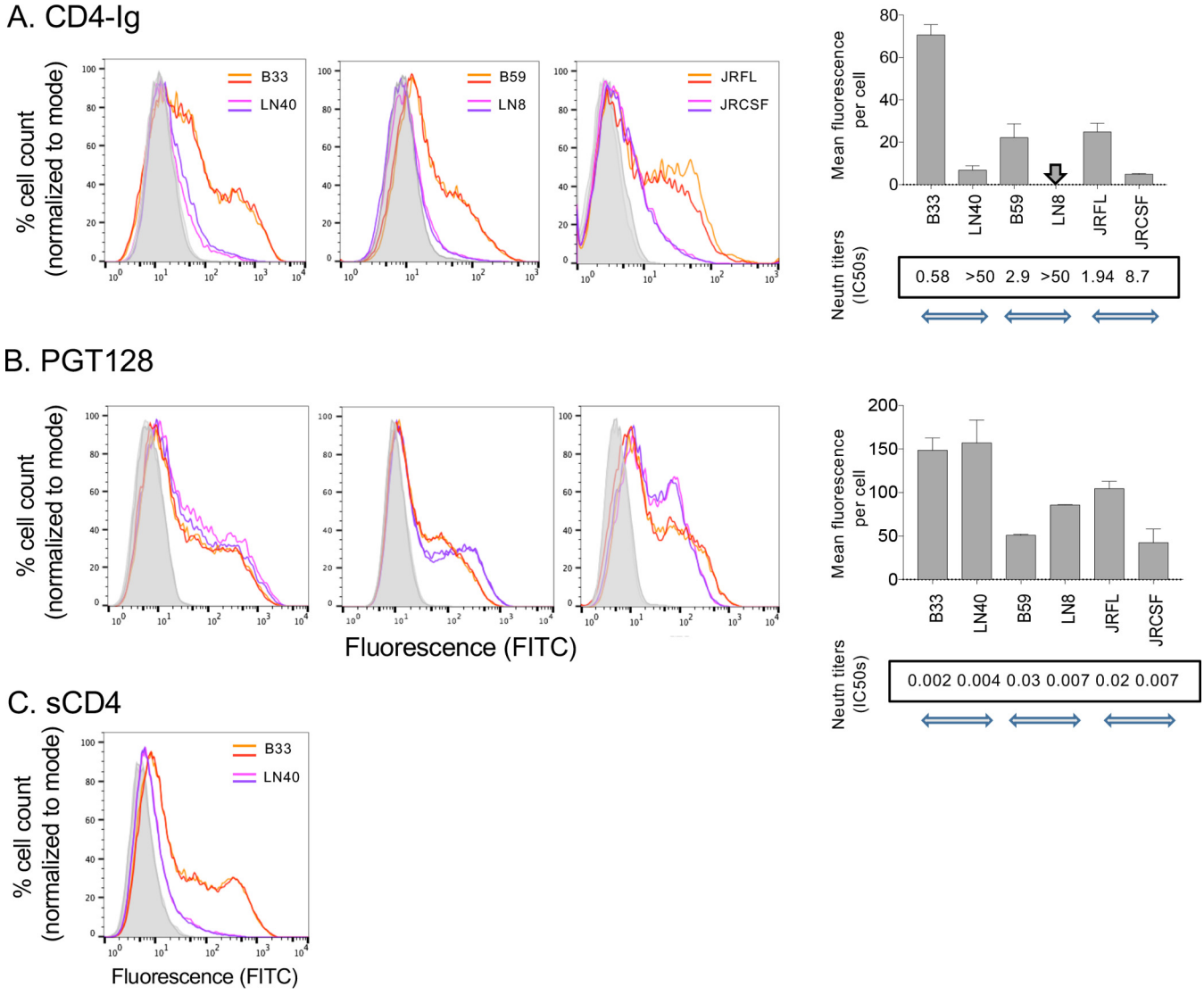

FIG 1 Trimeric Env binding to CD4-Ig. (A) Binding of CD4-Ig to Env trimers expressed on 293T cells measured by flow cytometry (left three graphs). Three Env pairs from different subjects were analyzed: B33 and LN40, B59 and LN8, and JRFL and JRCSF. Results for Envs from each pair were plotted in each of the three graphs presented, and each included a mac-tropic (B33, B59, or JRFL) and non-mac-tropic (LN40, LN8, or JRCSF) Env. Duplicate flow cytometry profiles for each Env are presented. CD4-Ig (10 μg/ml) binding to B33, B59, and JRFL Env trimers was readily detected. Binding to non-mac-tropic R5 Envs was at background levels. The rightmost graphs show mean fluorescence values plotted from data shown in the flow cytometry profiles. Boxed values at the bottom of each graph show CD4-Ig neutralization values (50% inhibitory concentrations [IC_{50}s], in micrograms per milliliter) of the equivalent Env^+ pseudoviruses. Horizontal arrows indicate the three Env pairs from three different patients. Vertical arrows indicate fluorescence measurements that were too low to register on the relevant graph. (B) All Envs bound efficiently to MAb PGT128, confirming efficient expression of both mac-tropic and non-mac-tropic Envs (left three graphs). The rightmost graphs show mean fluorescence values, with boxed values at the bottom of each graph indicating PGT128 neutralization titers of the equivalent Env^+ pseudoviruses as described for panel A. (C) Soluble CD4 binding to NA420 B33 and LN40 Envs, confirming that binding was similar to that observed for CD4-Ig as shown in panel A.

RESULTS

Trimeric mac-tropic Envs bind CD4-IgG efficiently, while binding for non-mac-tropic Envs is barely detectable. (i) Expression of HIV-1 Envs on 293T cells and CD4-Ig binding. We investigated the capacity of CD4-IgG to bind to trimeric Envs expressed on the surface of 293T cells. We expressed mac-tropic B33, B59, and JRFL and non-mac-tropic LN40, LN8, and JRCSF Envs on 293T cells and tested CD4-Ig binding (10 μg/ml). Envs in pSVIIIenv were cotransfected with pSV2-tat 72 and the furin expression vector pFurin into 293T cells (27). Overexpression of furin facilitates Env cleavage and the production of functional trimers (27). Env expression was modest but readily detected by MAbs and was quantifiable using flow cytometry. Figure 1A (left three

graphs) shows that mac-tropic Envs B33, B59, and JRFL bound efficiently to CD4-Ig, while for non-mac-tropic Envs LN40, LN8, and JRCSF, binding was at best very weak or undetectable. In contrast to CD4-Ig binding, all six Envs bound MAb PGT128, indicating that the lack of CD4-Ig binding for non-mac-tropic LN40, LN8, and JRCSF was not due to lack of expression (Fig. 1B, left three graphs). Of note, CD4-Ig and PGT128 binding to Envs on 293T cells broadly tracked with Env sensitivity to inhibition or neutralization by these reagents using Env^+ pseudoviruses carrying each of the six Envs (Fig. 1, rightmost graphs, where flow binding measurements are summarized, along with inhibition or neutralization titers). The only exception was JRCSF, which was neutralized by CD4-Ig with modest sensitivity, even though CD4-Ig binding to Envs expressed on 293T cells was at background levels.

Experiments so far tested CD4-Ig binding to Envs on 293T cells. CD4-Ig carries two D1D2 domains on CD4 and is thus dimeric (28). We next confirmed that monomeric soluble CD4 (sCD4) binding to Env trimers followed the same pattern of binding to 293T expressed Envs. We used B33 mac-tropic and LN40 non-mac-tropic Envs (Fig. 1C) and observed highly efficient binding to mac-tropic B33 but only background binding to non-mac-tropic LN40 Env, observations that parallel those for CD4-Ig (Fig. 1A, leftmost graph).

(ii) Expression of HIV-1 Envs on 293T cells and binding of a panel of human MAbs. We next tested Env binding to a further panel of eight MAbs to confirm efficient expression of each Env and to assess the presence of cleaved, native trimers. We wanted to compare MAb binding to each Env expressed on 293T cells, with neutralization titers obtained using Env^+ pseudoviruses to assess how closely 293T expressed Envs represented functional Envs on pseudoviruses. Flow cytometry profiles of MAb binding to each Env are presented in the left three graphs in each panel of Fig. 2, while a summary graph of binding measurements compared to neutralization is shown in the rightmost graphs. All Envs bound and were neutralized by 2G12 except B33, which lacks the glycan epitope for this MAb (29) (Fig. 2A). Env binding to trimer apex MAbs PG9 and PGT145 also followed the sensitivity of Env^+ pseudoviruses to neutralization (Fig. 2B and C). For example, non-mac-tropic Envs LN8 and JRCSF were efficiently bound by and neutralized by PG9 and PGT145, while LN40 (which lacks the N160 glycan required for binding [30]) did not bind these MAbs and was resistant to neutralization by them.

Only B33 Env bound V3 MAb 447-52D, and B33 is the only Env sensitive to neutralization by this MAb, thus confirming exposure of the V3 loop crown (16) (Fig. 2D). None of the Envs bound the CD4i MAb 17b on 293T cells, and all were resistant to neutralization by this MAb, consistent with the occlusion of CD4i and coreceptor binding site on native trimeric Envs (Fig. 2E).

Env binding to CD4bs MAbs VRC01, b12, and b6 was also tested (Fig. 2F to H). All Envs bound and were neutralized by VRC01, as expected for this broadly neutralizing antibody (31). However, b12 preferentially bound mac-tropic Envs that were sensitive to neutralization by this MAb (16). In contrast, none of the Envs efficiently bound or were neutralized by MAb b6, which is protected within primary trimeric Envs (16, 27).

For most MAbs and Envs, binding measured by flow (mean fluorescence) correlated with neutralization or inhibition titer (Table 1), although correlations were not apparent for CD4-Ig or MAbs b12 and PGT128. Nevertheless, whenever MAb binding was strong by flow, there was also sensitive neutralization. These data therefore support the expression of native Env trimers on 293T cells that mimic those present on virus particles during cell entry. There were a small number of exceptions, where binding and neutralization measurements were conflicting. These included CD4-Ig and JRCSF Env, where modest inhibition was apparent, but binding to Env^+ 293T cells was at best weak. Similarly, MAb b12 neutralized LN8, while binding to LN8 Env on 293T cells was very weak. The explanation for these discrepancies is unclear. There may be some situations where Env processing during and after the budding of virions alters the exposure of some epitopes (32–34). Alternatively, it is possible that the CD4bs on JRCSF

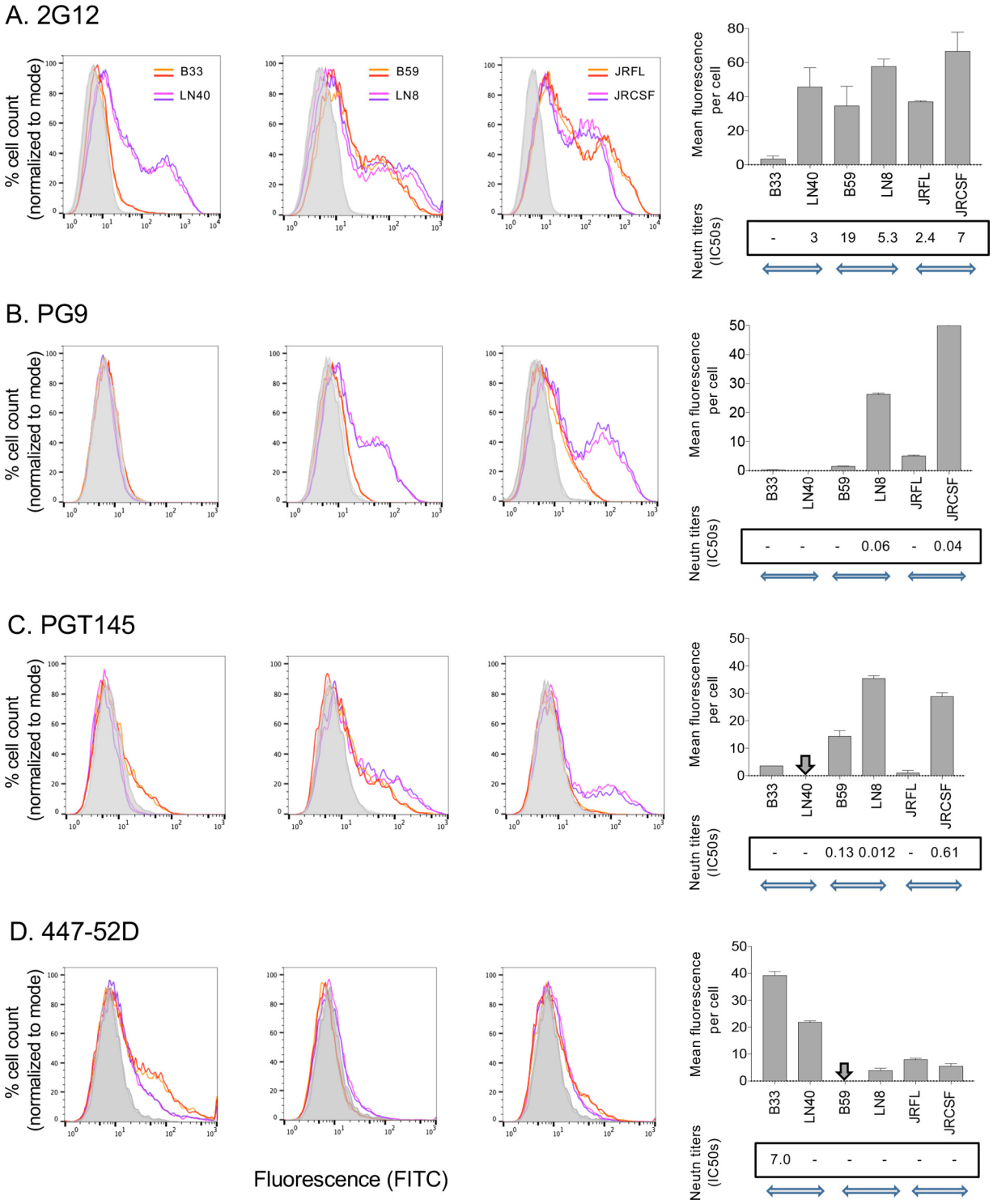

FIG 2 Flow cytometry showing MAb binding to Env trimers expressed on 293T cells. Human MAb binding to mac-tropic and non-mac-tropic R5 Env pairs: B33 and LN40, B59 and LN8, and JRFL and JRCSF. MAbs tested were 2G12 (A), PG9 (B), PG145 (C), 447-52D (D), 17b (E), VRC01 (F), b12 (G), and b6 (H). Duplicate flow cytometry profiles for each Env and MAb are presented. The rightmost graphs show mean fluorescence values plotted from data shown in the flow cytometry profiles. Boxed values at the bottom of each graph show CD4-Ig neutralization of the equivalent Env^+ pseudoviruses. Horizontal arrows indicate the three Env pairs from three different patients. Vertical arrows indicate fluorescence measurements that were too low to register on the relevant graph. MAb binding to trimers broadly tracked neutralization sensitivity, consistent with the expression and detection of functional Env trimers expressed on 293T cells (Table 2).

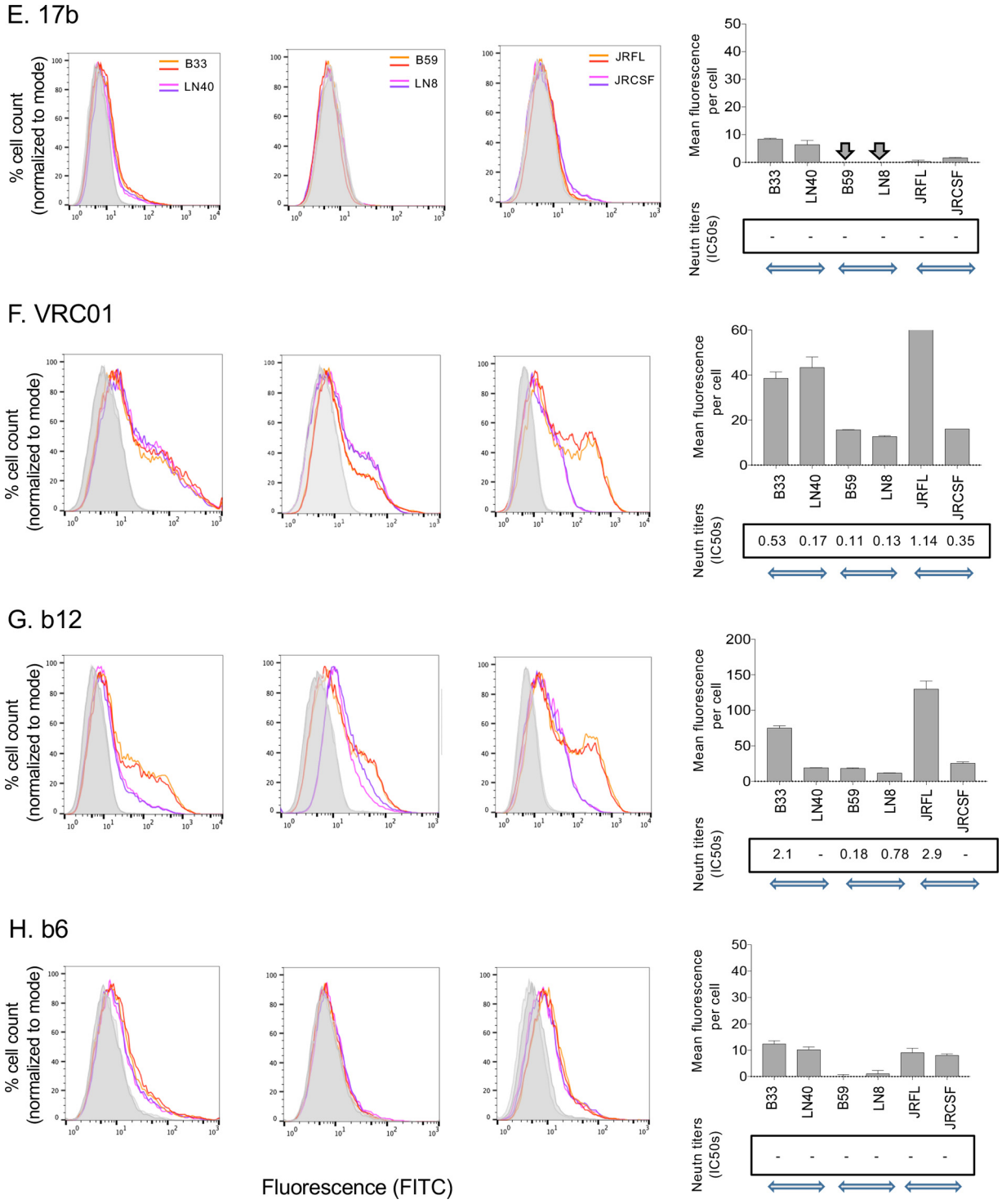

FIG 2 (Continued)

and the b12 epitope on LN8 become available at an undefined stage during entry into cells, allowing CD4-Ig and b12 to neutralize, respectively.

(iii) CD4 and MAb binding to soluble gp120. Undetectable binding of CD4-Ig to non-mac-tropic Env trimers is curious considering that these Envs routinely confer infection of $CD4^+$ cells where entry can be blocked by CD4-specific MAbs (35). To confirm that the Envs used in this current study bound CD4, we expressed gp120 in

TABLE 1 Correlations between binding and neutralization by CD4-Ig and MAbs to Envs expressed on 293T cells

MAb	Epitope(s)	Correlation between binding and neutralization	
		P value	Significance
CD4-Ig	CD4bs	0.19	
PGT128	V3/glycans	0.26	
2G12	Glycans	0.035	*
PG9	TAD apex	0.008	**
PGT145	TAD apex	0.016	*
447-52D	V3 loop	0.032	*
VRC01	CD4bs	0.01	**
b12	CD4bs	0.4726	
b6	CD4bs	—[a]	—
17b	CD4i	—	—

[a]A dash indicates that the antibody showed no binding and no neutralization. *, $P \leq 0.05$; **, $P \leq 0.01$.

soluble form and assessed binding to CD4-Ig using a Fortebio Octet QK^e platform. Results presented in Table 2 indicate that both mac-tropic and non-mac-tropic Envs bound CD4-Ig to high affinity in the low nanomolar range. Mac-tropic B33 and B59 gp120s conferred slightly higher affinities than did non-mac-tropic LN40 and LN8 gp120s, which were derived from subjects NA420 and NA20, respectively. In contrast, equilibrium dissociation constants (K_Ds) for gp120s from JRFL and JRCSF were not significantly different.

The lack of MAb binding to Envs expressed on 293T cells (Fig. 2) may result from the occlusion of the target epitopes within the trimer, or simply because the epitope is absent. This is an important issue for MAbs 447-52D, b12, b6, and 17b, because we are arguing that the epitopes for these MAbs are occluded within the trimer for the Envs that they do not bind. Previously, we used enzyme-linked immunosorbent assays (ELISAs) to test whether MAbs 447-52D and b12 bound to soluble gp120 derived from each of the Envs investigated in this work (16) and have now also tested MAbs 17b and b6 (data summarized in Table 2). We showed strong binding of both b6 and 17b (in the presence of sCD4) to gp120 by ELISAs. Together, these data show that all four MAbs bound to gp120s of all six Envs. The only exception was 17b binding to LN8 gp120, which was weak. This control experiment confirms that all six Envs under study carried b6, 17b, 447-52D, and b12 epitopes and supports the view that the lack of trimer binding for these MAbs is due to the occlusion of their epitopes. Again, these data support the expression of native, cleaved trimers rather than other Env products where the epitopes of these MAbs are potentially exposed.

(iv) Titration of CD4-IgG binding to mac-tropic and non-mac-tropic R5 Envs on 293T cells. We tested whether CD4-IgG binding to mac-tropic Envs expressed on 293T cells could be titrated out. For this experiment, we tested B33 and LN40 along with JRFL

TABLE 2 Soluble CD4 binding to CD4-Ig and human monoclonal antibodies[a]

Envs	Subject	CD4-Ig binding to gp120 KD	mab binding EC50s[1] μg/ml			
			b6	b12	447-52D	17b[2]
B33	NA420	2.8	0.021	0.018	0.001	0.055
LN40		16.1	0.021	0.023	0.001	0.2
B59	NA20	6.8	0.058	0.007	0.09	0.3
LN8		14.3	0.067	0.011	0.0007	6.0
JR-FL	JR	10.2	0.017	0.003	0.001	0.04
JR-CSF		12.9	0.014	0.002	0.0009	0.073

[a]CD4-Ig binding to soluble gp120 was measured by the ForteBio Octet QK^e platform (shown as K_Ds). MAb binding to gp120 was measured by ELISAs (shown as half-maximal effective concentrations [EC_{50}]). 1, color coding is as follows: red, <0.01 μg/ml; yellow, 0.01 to 0.1 μg/ml; orange, 0.1 to 1 μg/ml; and blue, >1 μg/ml. 2, 17b tested in the presence of sCD4 (3 μg/ml).

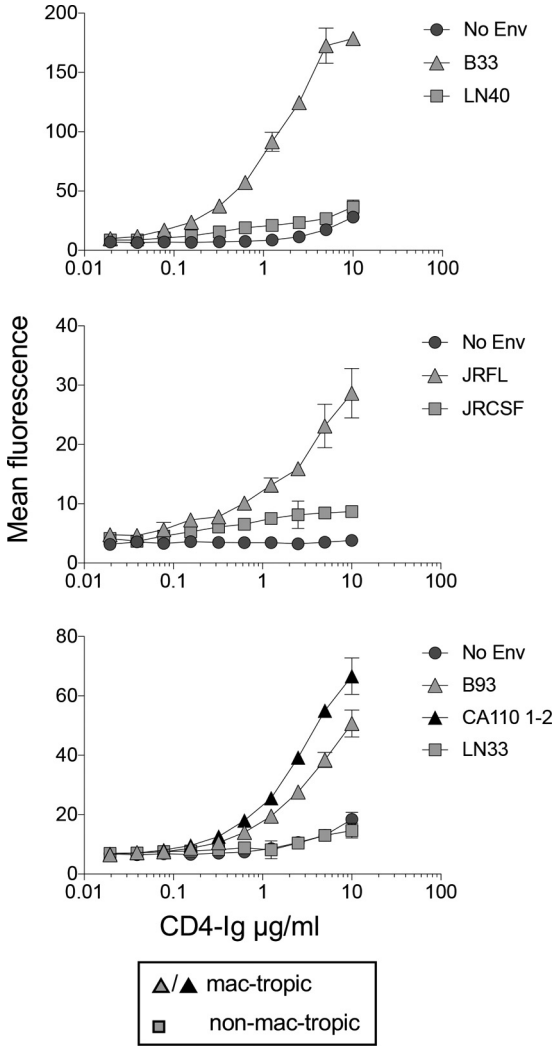

FIG 3 Titration of CD4-Ig binding to Env trimers. CD4-Ig binding to mac-tropic and non-mac-tropic R5 Envs was titrated out. Mac-tropic B33, JRFL, B93, and CA110 1-2 Env binding to CD4-Ig was detectable at <1 μg/ml, while binding to non-mac-tropic Envs LN40 and LN33 was undetectable at 10 μg/ml. However, weak, low-level binding of CD4-Ig to non-mac-tropic JRCSF was apparent.

and JRCSF, two Env pairs from subjects NA420 and JR, respectively (2, 3, 36). We also tested additional mac-tropic Envs, B93 and CA110 1-2, from brain tissue of subjects NA176 and CA110, respectively, as well as a non-mac-tropic Env, LN33, from lymph node tissue of subject NA118 (2, 37). The highest concentration of CD4-Ig tested was 10 μg/ml since higher concentrations resulted in an increase in nonspecific background staining.

Figure 3 shows binding curves for each Env. For each of the four mac-tropic Envs, CD4-Ig binding could be titrated out, with positive staining still detectable at between 0.3 and 0.6 μg/ml of CD4-Ig (Fig. 3). In contrast, CD4-IgG binding to non-mac-tropic Envs, LN40 and LN33, was not detected even at 10 μg/ml, while binding to JRCSF was low to background across several CD4-Ig concentrations, including 10 μg/ml. We were unable to measure half-maximal binding of CD4-Ig concentrations for mac-tropic Envs, since it was unclear whether maximal binding had been achieved at 10 μg/ml.

In summary, CD4-IgG bound efficiently to mac-tropic R5 Envs expressed on 293T cells, while binding to non-mac-tropic Envs was at best barely detectable. Binding to mac-tropic R5 Envs was at least 15- to 30-fold higher than for non-mac-tropic Envs.

Soluble CD4 treatment of non-mac-tropic LN8 Env does not modulate the V2q (PGT145) epitope or expose the V3 loop crown. It seemed surprising that CD4-IgG

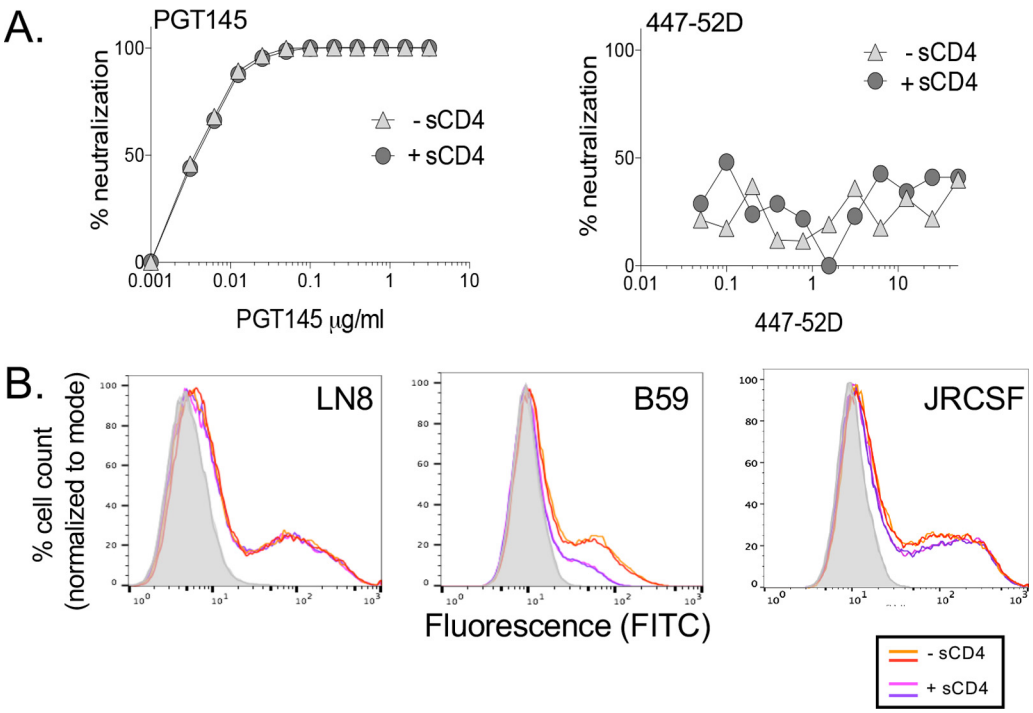

FIG 4 High concentrations of sCD4 do not modulate trimer association domain MAb PGT145 or V3 crown MAb 447-52D epitopes on R5 non-mac-tropic Env LN8. (A) (Left) The high sensitivity of LN8 Env$^+$ pseudoviruses to MAb PGT145 neutralization was not affected by pretreatment and the presence of 25 μg/ml sCD4. (Right) Pretreatment and the presence of 25 μg/ml of sCD4 failed to expose the 447-52D epitope on the V3 crown of LN8. (B) Soluble CD4 (20 μg/ml) failed to modulate the PGT145 TAD epitope on non-mac-tropic Envs LN8 (left) and JRCSF (right), consistent with the lack of CD4 binding. In contrast, sCD4 downregulated the PGT145 epitope for mac-tropic Env B59 (middle), consistent with CD4 binding and TAD opening. Note that the 447-52D epitope is present on LN8 Env but occluded on the trimer (16).

(10 μg/ml) binding to non-mac-tropic R5 Env trimers was not reliably detected, considering that all primary HIV-1 Envs require cell surface CD4 to trigger entry. However, non-mac-tropic R5 Env$^+$ viruses are also generally resistant to inhibition by sCD4, which could be consistent with a lack of binding. However, it is also possible that sCD4 may bind to non-mac-tropic Envs and initiate conformational changes that fail to complete and result in sCD4 falling off. In this situation, it should be possible to observe changes in the TAD structure in the presence of sCD4. To test this, we investigated whether sCD4 treatment of pseudoviruses carrying non-mac-tropic LN8 Envs modulated the PGT145 (TAD, V2q) or 447-52D (V3) epitopes on Env. These two MAbs were appropriate for this experiment since we had previously shown that LN8 Env$^+$ pseudoviruses were highly sensitive to PG9/PG16-type MAbs (16). In contrast, while LN8 gp120 bound 447-52D with an extremely low half-maximal effective concentration (EC_{50}) (Table 2), Env$^+$ pseudoviruses were resistant to neutralization. If sCD4 could bind to LN8 Envs and induce conformational changes in the trimer, we would expect to observe loss of the PGT145 epitope and, at the same time, exposure of the V3 loop and 447-52D epitope. Figure 4A shows that LN8 Env$^+$ pseudovirions remained sensitive to PGT145 and resistant to 447-52D MAbs even in the presence of 25 μg/ml of sCD4. We also confirmed that sCD4 failed to modulate the PGT145 epitope on both LN8 and JRCSF by testing MAb binding to trimers expressed on 293T cells (Fig. 4B). In contrast, sCD4 significantly reduced PGT145 binding to mac-tropic B59 Env trimers. Together, these results are consistent with a lack of sCD4 binding to LN8 and JRCSF Env trimers and support the lack of binding by CD4-IgG observed in the trimer binding assay (Fig. 1 and 3).

DISCUSSION

We demonstrate that mac-tropic R5 Env trimers have higher affinity for CD4 than do non-mac-tropic R5 Envs. Remarkably, CD4 binding for non-mac-tropic Envs trimers

derived from lymph node tissue was undetectable despite high-affinity binding of CD4 by soluble gp120s from the same Envs. Together, these data indicate that the CD4bs on non-mac-tropic R5 Env trimers from immune tissue is occluded, presumably to protect against binding of CD4bs antibodies. These data confirm for native trimeric Envs several previous observations that implied a higher CD4 affinity for mac-tropic Envs, including (i) infection of cells carrying low levels of CD4 (2, 3, 5, 24, 38), (ii) high sensitivity to inhibition by sCD4 (35), (iii) determinants of mac tropism within or proximal to the CD4bs (21, 22), and (iv) a higher gp120-CD4 affinity for mac-tropic Envs carrying N283 determinant in the CD4bs (21).

Expression of HIV-1 Envs on 293T and other cell types results in several nonfunctional forms of Env reaching the cell surface. These include uncleaved gp160 trimers (39–41), soluble forms of gp160 (42, 43), gp41 stumps (42), and shed gp120 monomers (44, 45). We investigated binding of Envs expressed on 293T cells to a panel of nine Env MAbs previously used to evaluate overall Env expression and the presence of mature, cleaved trimers (27). Briefly, the lack of binding by the CD4bs MAb, b6, supports the presence of closed and cleaved trimers since this MAb binds a CD4bs epitope that is protected within mature trimers but would be exposed on gp120 monomers and uncleaved Envs. Similarly, the lack of binding by CD4i MAb 17b supports the presence of untriggered trimers. In addition, binding of the different MAbs tracked closely to neutralization data supporting the presence of functional trimers. Of note, the lack of CD4-IgG binding to non-mac-tropic Envs also supports the presence of cleaved trimers for these Envs, since uncleaved Envs, monomers and/or defective Envs would be expected to carry a more exposed CD4bs and to bind CD4-IgG more efficiently (27).

Our study is based on a relatively small sample of mac-tropic and non-mac-tropic R5 Envs. However, we expect that the results presented on Env-receptor interactions will apply to many Envs of these tropisms. This is because our previous studies on many other such Envs have shown a clear consistency on sensitivity to reagents that block or inhibit Env-receptor interactions, including sCD4 and CD4-Ig and anti-CD4 MAbs and CCR5 antagonists (2, 3, 16, 30, 35, 37, 46). Together, these studies indicate that mac-tropic and non-mac-tropic Env groups each share their own common receptor binding characteristics.

Non-mac-tropic Env trimers did not convincingly bind CD4-Ig or sCD4. We expressed soluble gp120 from these Envs and confirmed that they bound CD4-Ig with high affinity. For this experiment, we used gp120 preparations produced on 293T cells that had been purified via lectin columns. This approach enabled multiple gp120 preparations to be produced routinely. However, Coutu and Finzi recently reported that soluble gp120 produced from 293T cells frequently contained unnatural dimers that affect estimates of gp120-CD4 affinities providing low measurements (47). The gp120 preparations used in this study contained variable amounts of dimers, from undetectable to just modest levels (data not shown). Regardless, each gp120 tested bound CD4 with high affinity, confirming that the non-mac-tropic Envs carried the potential to bind CD4.

Weak or undetectable binding of CD4 for non-mac-tropic R5 Envs is remarkable. How do these non-mac-tropic Envs trigger infection of $CD4^+$ T cells if CD4 binding is so inefficient? $CD4^+$ T cells carry high concentrations of CD4 (20), which may help compensate. However, non-mac-tropic Env^+ viruses may preferentially infect via virological synapses where both CD4 and CCR5 become highly concentrated on the T-cell target membrane present in synapses, while Env is concentrated on the membrane of the infected cell. Previously, we reported that *trans*-infection of $CD4^+$ T cells across synapses by virus captured by monocyte-derived dendritic cells preferentially supported infection by non-mac-tropic Env^+ pseudoviruses, consistent with this hypothesis (26). It is therefore likely that the high density of Envs meeting a high density of receptors in the synapse enables high-avidity interactions that can overcome low Env-CD4 affinities.

MATERIALS AND METHODS

Envelope clones. Full-length HIV-1 Env clones were expressed from pSVIIIenv or from Rev-Env inserts in pcDNA3.1 as previously reported (16). JRFL and JRCSF Env clones were codon optimized and expressed from pcDNA3.1.

gp120s were expressed from pJW4303 as previously described (16, 48). gp120 sequences were cloned into pJW4303 downstream of the tissue plasminogen activator (tPA) leader sequence.

The GenBank accession numbers for envelopes used are as follows: NA420 B33, GU724973; NA420 LN40, GU724974; NA20 B59, HM014318; NA20 LN8, HM014322; JRFL, U63632; JRCSF, AY426126; NA118 LN33, HM771419; and CA110 1-2, MF975654.

Cells. Cells used have all been described previously and included HeLa TZM-bl (49) and 293T and 293F (50–52) cells.

Authentication of cell lines. HeLa TZM-bl cells were obtained from the NIH AIDS Reagent Program and stored frozen at an early passage. These cells are susceptible to R5 and X4 HIV-1 strains and express β-galactosidase and luciferase when infected by HIV. The early-passage cells used in this study exhibited this susceptibility phenotype, helping to confirm their authenticity. 293T/17 cells were obtained from the ATCC and FreeStyle 293F cells from Thermo Fisher Scientific Inc. These cells have been kept frozen since an early passage. 293F cells were successfully used to produce gp120, CD4-Ig, and some monoclonal antibodies. 293T cells were used to express native HIV-1 Envs on the cell surface for CD4-Ig and antibody binding assays as well as to produce HIV-1 Env$^+$ pseudovirus stocks following transfection of appropriate plasmid DNA constructs. The consistent high infectivity titers of these Env$^+$ pseudoviruses produced from 293T cells, which exhibit predicted Env tropisms and properties, help to verify their authenticity.

Preparation of soluble gp120 and CD4-Ig. Suspension 293F cells (1×10^6/ml in 500 ml) were transfected with 250 μg of DNA of pJW4303 containing different gp120s (48) using suspension 293Fectin (Invitrogen Inc.) according to the manufacturer's instructions. Transfected cells were cultured in Freestyle 293 expression medium (Invitrogen Inc.) in shaking flasks for 72 h. Cells were then centrifuged out and supernatants harvested before purifying gp120 over a lectin column. Then gp120s were concentrated with 50,000 (50K)-molecular-weight (MW)-cutoff centrifugal filter concentrators (Millipore Inc.).

Similarly, 250 μg of DNA of pcDM8 encoding CD4-Ig (53) was transfected into 293F cells (1×10^6/ml in 500 ml) using suspension 293Fectin (Invitrogen Inc.). Following 3 days of culture, supernatant carrying CD4-Ig was harvested, concentrated using tangential-flow filtration with a 70-kDa cutoff, and purified with protein G Sepharose.

Soluble gp120/CD4 binding and affinity measurements. Soluble gp120 binding to CD4-Ig was investigated using a ForteBio Octet QK^e platform according to the manufacturer's instructions. This approach exploits biolayer interferometry (BLI) measurements to detect binding in a 96-well plate format. Protein A-coated biosensors were loaded with CD4-Ig (10 μg/ml) in phosphate-buffered saline (PBS), 0.1% bovine serum albumin (BSA), 0.02% Tween 20, and 0.05% sodium azide. After capture, sensors were washed in loading buffer to remove excess unbound CD4-Ig so that a new baseline signal was established. The biosensors were then put into wells containing the different gp120 proteins at 2-fold serially diluted concentrations from 300 to 18.8 nM in loading buffer for 10 min to measure binding rates (k_{on}). Sensors were then placed into wells containing loading buffer without gp120 to measure dissociation over 10 min (k_{off}). Equilibrium dissociation constant (K_D) values were calculated as the ratio of k_{off} to k_{on} values using the ForteBio Octet QK^e data analysis software, package 7.1, via a 1:1 binding model with the local fitting function followed by the global fitting function.

Expression and detection of Env trimers on 293T cells. A total of 2×10^5 293T cells were seeded per well of 6-well plates the day before transfection. A transfection mix containing 25 μg of DNA of each of Env$^+$ pSVIIIenv and pSV-tat72 together with 25 μg of pFurin (27) with Fugene6 in Opti-MEM was prepared to a total of 1.875 ml. This was sufficient to transfect 12×10^5 293T cells according to the manufacturer's protocol.

Following 2 days of culture, transfected cells were detached using Versene and used for MAb staining or CD4-IgG binding. A total of 0.5×10^6 cells were seeded into 96-well V-bottom plates and treated with appropriate MAb or CD4-Ig concentrations in Dulbecco modified Eagle medium (DMEM) (4% fetal calf serum [FCS]) for 40 min at 37°C. Cells were then washed in PBS and 1% FCS and treated with goat-anti-human IgG-fluorescein isothiocyanate (FITC) conjugate (Southern Biotech Inc.) for 40 min at room temperature (RT), washed again in PBS, 1% FCS, and then PBS, and fixed in 4% formaldehyde in PBS. Fixed cells from each well were then filtered through a 35-μm filter-capped tube (Falcon Inc.) and analyzed by flow cytometry in the UMASS Medical School Flow Cytometry Core Lab. Experiments were done in duplicate and at least twice, frequently multiple times. The results of one representative experiment are presented, with duplicates shown. Fluorescence measurements for each Env varied in different experiments due to differences in the efficiency of each transfection (of DNA clones for Env expression). For these experiments, we were most concerned with variation in CD4-Ig binding rather than transfection efficiency, so we did not compare results between experiments.

CD4-Ig is a chimeric molecule comprising part immunoglobulin and part CD4. CD4-Ig has two CD4 molecules (two domains each) and is therefore dimeric for CD4 (28). We also tested monomeric sCD4 (four domains) for its capacity to bind to mac-tropic B33 and non-mac-tropic LN40 Envs and obtained results similar to those for CD4-Ig (Fig. 1C). This was achieved by staining with the CD4 MAb OKT4, followed by a goat anti-mouse IgG-FITC conjugate (Southern Biotech Inc.). However, the assay using sCD4 was less consistent and had higher background than that with CD4-Ig, probably due to the additional layer of a mouse-anti-CD4 MAb that was required. We therefore persisted with assays using CD4-Ig.

Measurement of monoclonal antibody binding to gp120 by ELISA. The binding of MAbs 17b (CD4i) and b6 (CD4bs) to gp120 was estimated using an ELISA protocol. ELISA data for MAbs b12 and 447-52D were taken from our previous publication (16).

Serial 2-fold dilutions of each MAb were added to captured gp120. A dilution of gp120 that saturated the capture antibody was used throughout (54). Costar 96-well ELISA plates (Corning Inc.) were coated with 250 ng/well of sheep anti-gp120 Ab D7324 (Aalto, Inc.) in phosphate-buffered saline (PBS). After overnight incubation at RT, plates were washed twice with PBS–0.05% Tween, incubated for 2 h at RT with blocking solution (3% bovine serum albumin in PBS), and washed four times with PBS–0.05% Tween. Soluble gp120 (4 μg/ml) was added for 120 min before washing 10 times and adding 2-fold dilutions of 17b and b6 MAbs for 1 h at RT. After 10 washes, 50 μl/well of goat anti-human immunoglobulin G, $F(ab')_2$ fragment-specific calf intestinal alkaline phosphatase conjugate (Pierce Inc.) diluted 1:1,000 in dilution buffer was added to plates. After 1 h of incubation at RT, 50 μl of 3,3′,5,5′-tetramethylbenzidine (TMB) substrate (eBioscience Inc.) was added to each well before adding 2 M sulfuric acid (stop solution) following color development. Plates were read at 492 nm, and EC_{50} values were calculated using GraphPad Prism.

Preparation and titration of Env$^+$ pseudoviruses. Env$^+$ pSVIIIenv was cotransfected into 293T cells with *env*$^-$ pNL43. Env$^+$ pseudovirions were harvested after 48 h, clarified by low-speed centrifugation, and frozen as aliquots at −152°C. Env$^+$ pseudovirions were titrated on HeLa TZM-bl cells, which carry β-galactosidase and luciferase reporter genes controlled by HIV long terminal repeat (LTR) promoters (49). Infected cells were visualized at 48 h after infection as focus-forming units (FFU) following staining for β-galactosidase activity. Since Env$^+$ pseudovirions are capable of only a single round of replication, individual cells or small groups of divided cells were counted as foci.

Neutralization assays. Neutralization assays were performed as described previously using HeLa TZM-bl cells and a luminescence readout (16).

Accession number(s). The CA110 1-2 sequence has been deposited in GenBank under accession number MF975654.

ACKNOWLEDGMENTS

We acknowledge the NIH AIDS Reagent Program and the Centre for AIDS Reagents, NIBSC, United Kingdom, for services and reagents.

This study was supported by NIH R01 grants AI089334, NS084910, and NS095749. J.L. is supported by R01 grant AI111809 and DP1 grant DA034990.

REFERENCES

1. Wilen CB, Tilton JC, Doms RW. 2012. Molecular mechanisms of HIV entry. Adv Exp Med Biol 726:223–242. https://doi.org/10.1007/978-1-4614-0980-9_10.
2. Peters PJ, Bhattacharya J, Hibbitts S, Dittmar MT, Simmons G, Bell J, Simmonds P, Clapham PR. 2004. Biological analysis of human immunodeficiency virus type 1 R5 envelopes amplified from brain and lymph node tissues of AIDS patients with neuropathology reveals two distinct tropism phenotypes and identifies envelopes in the brain that confer an enhanced tropism and fusigenicity for macrophages. J Virol 78:6915–6926. https://doi.org/10.1128/JVI.78.13.6915-6926.2004.
3. Peters PJ, Sullivan WM, Duenas-Decamp MJ, Bhattacharya J, Ankghuambom C, Brown R, Luzuriaga K, Bell J, Simmonds P, Ball J, Clapham PR. 2006. Non-macrophage-tropic human immunodeficiency virus type 1 R5 envelopes predominate in blood, lymph nodes, and semen: implications for transmission and pathogenesis. J Virol 80:6324–6332. https://doi.org/10.1128/JVI.02328-05.
4. Sturdevant CB, Joseph SB, Schnell G, Price RW, Swanstrom R, Spudich S. 2015. Compartmentalized replication of R5 T cell-tropic HIV-1 in the central nervous system early in the course of infection. PLoS Pathog 11:e1004720. https://doi.org/10.1371/journal.ppat.1004720.
5. Schnell G, Joseph S, Spudich S, Price RW, Swanstrom R. 2011. HIV-1 replication in the central nervous system occurs in two distinct cell types. PLoS Pathog 7:e1002286. https://doi.org/10.1371/journal.ppat.1002286.
6. Brown RJ, Peters PJ, Caron C, Gonzalez-Perez MP, Stones L, Ankghuambom C, Pondei K, McClure CP, Alemnji G, Taylor S, Sharp PM, Clapham PR, Ball JK. 2011. Intercompartmental recombination of HIV-1 contributes to env intrahost diversity and modulates viral tropism and sensitivity to entry inhibitors. J Virol 85:6024–6037. https://doi.org/10.1128/JVI.00131-11.
7. Bednar MM, Hauser BM, Ping LH, Dukhovlinova E, Zhou S, Arrildt KT, Hoffman IF, Eron JJ, Cohen MS, Swanstrom R. 2015. R5 macrophage-tropic HIV-1 in the male genital tract. J Virol 89:10688–10692. https://doi.org/10.1128/JVI.01842-15.
8. Julien JP, Cupo A, Sok D, Stanfield RL, Lyumkis D, Deller MC, Klasse PJ, Burton DR, Sanders RW, Moore JP, Ward AB, Wilson IA. 2013. Crystal structure of a soluble cleaved HIV-1 envelope trimer. Science 342:1477–1483. https://doi.org/10.1126/science.1245625.
9. Lyumkis D, Julien JP, de Val N, Cupo A, Potter CS, Klasse PJ, Burton DR, Sanders RW, Moore JP, Carragher B, Wilson IA, Ward AB. 2013. Cryo-EM structure of a fully glycosylated soluble cleaved HIV-1 envelope trimer. Science 342:1484–1490. https://doi.org/10.1126/science.1245627.
10. Bartesaghi A, Merk A, Borgnia MJ, Milne JL, Subramaniam S. 2013. Prefusion structure of trimeric HIV-1 envelope glycoprotein determined by cryo-electron microscopy. Nat Struct Mol Biol 20:1352–1357. https://doi.org/10.1038/nsmb.2711.
11. Pancera M, Zhou T, Druz A, Georgiev IS, Soto C, Gorman J, Huang J, Acharya P, Chuang GY, Ofek G, Stewart-Jones GB, Stuckey J, Bailer RT, Joyce MG, Louder MK, Tumba N, Yang Y, Zhang B, Cohen MS, Haynes BF, Mascola JR, Morris L, Munro JB, Blanchard SC, Mothes W, Connors M, Kwong PD. 2014. Structure and immune recognition of trimeric pre-fusion HIV-1 Env. Nature 514:455–461. https://doi.org/10.1038/nature13808.
12. Julien JP, Lee JH, Ozorowski G, Hua Y, Torrents de la Pena A, de Taeye SW, Nieusma T, Cupo A, Yasmeen A, Golabek M, Pugach P, Klasse PJ, Moore JP, Sanders RW, Ward AB, Wilson IA. 2015. Design and structure of two HIV-1 clade C SOSIP.664 trimers that increase the arsenal of native-like Env immunogens. Proc Natl Acad Sci U S A 112:11947–11952. https://doi.org/10.1073/pnas.1507793112.
13. Pugach P, Ozorowski G, Cupo A, Ringe R, Yasmeen A, de Val N, Derking R, Kim HJ, Korzun J, Golabek M, de Los Reyes K, Ketas TJ, Julien JP, Burton DR, Wilson IA, Sanders RW, Klasse PJ, Ward AB, Moore JP. 2015. A native-like SOSIP.664 trimer based on an HIV-1 subtype B env gene. J Virol 89:3380–3395. https://doi.org/10.1128/JVI.03473-14.
14. Kwon YD, Pancera M, Acharya P, Georgiev IS, Crooks ET, Gorman J, Joyce MG, Guttman M, Ma X, Narpala S, Soto C, Terry DS, Yang Y, Zhou T, Ahlsen G, Bailer RT, Chambers M, Chuang GY, Doria-Rose NA, Druz A, Hallen MA, Harned A, Kirys T, Louder MK, O'Dell S, Ofek G, Osawa K, Prabhakaran M, Sastry M, Stewart-Jones GB, Stuckey J, Thomas PV, Tittley T, Williams C, Zhang B, Zhao H, Zhou Z, Donald BR, Lee LK, Zolla-Pazner S, Baxa U, Schon A, Freire E, Shapiro L, Lee KK, Arthos J, Munro JB, Blanchard SC, Mothes W, Binley JM, McDermott AB, Mascola

JR, Kwong PD. 2015. Crystal structure, conformational fixation and entry-related interactions of mature ligand-free HIV-1 Env. Nat Struct Mol Biol 22:522–531. https://doi.org/10.1038/nsmb.3051.
15. Harris A, Borgnia MJ, Shi D, Bartesaghi A, He H, Pejchal R, Kang YK, Depetris R, Marozsan AJ, Sanders RW, Klasse PJ, Milne JL, Wilson IA, Olson WC, Moore JP, Subramaniam S. 2011. Trimeric HIV-1 glycoprotein gp140 immunogens and native HIV-1 envelope glycoproteins display the same closed and open quaternary molecular architectures. Proc Natl Acad Sci U S A 108:11440–11445. https://doi.org/10.1073/pnas.1101414108.
16. O'Connell O, Repik A, Reeves JD, Gonzalez-Perez MP, Quitadamo B, Anton ED, Duenas-Decamp M, Peters P, Lin R, Zolla-Pazner S, Corti D, Wallace A, Wang S, Kong XP, Lu S, Clapham PR. 2013. Efficiency of bridging-sheet recruitment explains HIV-1 R5 envelope glycoprotein sensitivity to soluble CD4 and macrophage tropism. J Virol 87:187–198. https://doi.org/10.1128/JVI.01834-12.
17. Burton DR, Hangartner L. 2016. Broadly neutralizing antibodies to HIV and their role in vaccine design. Annu Rev Immunol 34:635–659. https://doi.org/10.1146/annurev-immunol-041015-055515.
18. Mori K, Rosenzweig M, Desrosiers RC. 2000. Mechanisms for adaptation of simian immunodeficiency virus to replication in alveolar macrophages. J Virol 74:10852–10859. https://doi.org/10.1128/JVI.74.22.10852-10859.2000.
19. Bannert N, Schenten D, Craig S, Sodroski J. 2000. The level of CD4 expression limits infection of primary rhesus monkey macrophages by a T-tropic simian immunodeficiency virus and macrophagetropic human immunodeficiency viruses. J Virol 74:10984–10993. https://doi.org/10.1128/JVI.74.23.10984-10993.2000.
20. Lee B, Sharron M, Montaner LJ, Weissman D, Doms RW. 1999. Quantification of CD4, CCR5, and CXCR4 levels on lymphocyte subsets, dendritic cells, and differentially conditioned monocyte-derived macrophages. Proc Natl Acad Sci U S A 96:5215–5220. https://doi.org/10.1073/pnas.96.9.5215.
21. Dunfee RL, Thomas ER, Gorry PR, Wang J, Taylor J, Kunstman K, Wolinsky SM, Gabuzda D. 2006. The HIV Env variant N283 enhances macrophage tropism and is associated with brain infection and dementia. Proc Natl Acad Sci U S A 103:15160–15165. https://doi.org/10.1073/pnas.0605513103.
22. Duenas-Decamp MJ, Peters PJ, Burton D, Clapham PR. 2009. Determinants flanking the CD4 binding loop modulate macrophage tropism of human immunodeficiency virus type 1 R5 envelopes. J Virol 83:2575–2583. https://doi.org/10.1128/JVI.02133-08.
23. Musich T, Peters PJ, Duenas-Decamp MJ, Gonzalez-Perez MP, Robinson J, Zolla-Pazner S, Ball JK, Luzuriaga K, Clapham PR. 2011. A conserved determinant in the V1 loop of HIV-1 modulates the V3 loop to prime low CD4 use and macrophage infection. J Virol 85:2397–2405. https://doi.org/10.1128/JVI.02187-10.
24. Walter BL, Wehrly K, Swanstrom R, Platt E, Kabat D, Chesebro B. 2005. Role of low CD4 levels in the influence of human immunodeficiency virus type 1 envelope V1 and V2 regions on entry and spread in macrophages. J Virol 79:4828–4837. https://doi.org/10.1128/JVI.79.8.4828-4837.2005.
25. Alvarez RA, Barria MI, Chen BK. 2014. Unique features of HIV-1 spread through T cell virological synapses. PLoS Pathog 10:e1004513. https://doi.org/10.1371/journal.ppat.1004513.
26. Musich T, O'Connell O, Gonzalez-Perez MP, Derdeyn CA, Peters PJ, Clapham PR. 2015. HIV-1 non-macrophage-tropic R5 envelope glycoproteins are not more tropic for entry into primary CD4+ T-cells than envelopes highly adapted for macrophages. Retrovirology 12:25. https://doi.org/10.1186/s12977-015-0141-0.
27. Ringe RP, Sanders RW, Yasmeen A, Kim HJ, Lee JH, Cupo A, Korzun J, Derking R, van Montfort T, Julien JP, Wilson IA, Klasse PJ, Ward AB, Moore JP. 2013. Cleavage strongly influences whether soluble HIV-1 envelope glycoprotein trimers adopt a native-like conformation. Proc Natl Acad Sci U S A 110:18256–18261. https://doi.org/10.1073/pnas.1314351110.
28. Gardner MR, Kattenhorn LM, Kondur HR, von Schaewen M, Dorfman T, Chiang JJ, Haworth KG, Decker JM, Alpert MD, Bailey CC, Neale ES, Jr, Fellinger CH, Joshi VR, Fuchs SP, Martinez-Navio JM, Quinlan BD, Yao AY, Mouquet H, Gorman J, Zhang B, Poignard P, Nussenzweig MC, Burton DR, Kwong PD, Piatak M, Jr, Lifson JD, Gao G, Desrosiers RC, Evans DT, Hahn BH, Ploss A, Cannon PM, Seaman MS, Farzan M. 2015. AAV-expressed eCD4-Ig provides durable protection from multiple SHIV challenges. Nature 519:87–91. https://doi.org/10.1038/nature14264.
29. Duenas-Decamp MJ, Clapham PR. 2010. HIV-1 gp120 determinants proximal to the CD4 binding site shift protective glycans that are targeted by monoclonal antibody, 2G12. J Virol 84:9608–9612. https://doi.org/10.1128/JVI.00185-10.
30. Duenas-Decamp M, Jiang L, Bolon D, Clapham PR. 2016. Saturation mutagenesis of the HIV-1 envelope CD4 binding loop reveals residues controlling distinct trimer conformations. PLoS Pathog 12:e1005988. https://doi.org/10.1371/journal.ppat.1005988.
31. Zhou T, Georgiev I, Wu X, Yang ZY, Dai K, Finzi A, Do Kwon Y, Scheid J, Shi W, Xu L, Yang Y, Zhu J, Nussenzweig MC, Sodroski J, Shapiro L, Nabel GJ, Mascola JR, Kwong PD. 2010. Structural basis for broad and potent neutralization of HIV-1 by antibody VRC01. Science 329:811–817. https://doi.org/10.1126/science.1192819.
32. Jiang J, Aiken C. 2007. Maturation-dependent human immunodeficiency virus type 1 particle fusion requires a carboxyl-terminal region of the gp41 cytoplasmic tail. J Virol 81:9999–10008. https://doi.org/10.1128/JVI.00592-07.
33. Murakami T, Ablan S, Freed EO, Tanaka Y. 2004. Regulation of human immunodeficiency virus type 1 Env-mediated membrane fusion by viral protease activity. J Virol 78:1026–1031. https://doi.org/10.1128/JVI.78.2.1026-1031.2004.
34. Wyma DJ, Jiang J, Shi J, Zhou J, Lineberger JE, Miller MD, Aiken C. 2004. Coupling of human immunodeficiency virus type 1 fusion to virion maturation: a novel role of the gp41 cytoplasmic tail. J Virol 78:3429–3435. https://doi.org/10.1128/JVI.78.7.3429-3435.2004.
35. Peters PJ, Duenas-Decamp MJ, Sullivan WM, Brown R, Ankghuambom C, Luzuriaga K, Robinson J, Burton DR, Bell J, Simmonds P, Ball J, Clapham P. 2008. Variation in HIV-1 R5 macrophage-tropism correlates with sensitivity to reagents that block envelope: CD4 interactions but not with sensitivity to other entry inhibitors. Retrovirology 5:5. https://doi.org/10.1186/1742-4690-5-5.
36. Koyanagi Y, Miles S, Mitsuyasu RT, Merrill JE, Vinters HV, Chen IS. 1987. Dual infection of the central nervous system by AIDS viruses with distinct cellular tropisms. Science 236:819–822. https://doi.org/10.1126/science.3646751.
37. Gonzalez-Perez MP, O'Connell O, Lin R, Sullivan WM, Bell J, Simmonds P, Clapham PR. 2012. Independent evolution of macrophage-tropism and increased charge between HIV-1 R5 envelopes present in brain and immune tissue. Retrovirology 9:20. https://doi.org/10.1186/1742-4690-9-20.
38. Thomas ER, Dunfee RL, Stanton J, Bogdan D, Taylor J, Kunstman K, Bell JE, Wolinsky SM, Gabuzda D. 2007. Macrophage entry mediated by HIV Envs from brain and lymphoid tissues is determined by the capacity to use low CD4 levels and overall efficiency of fusion. Virology 360:105–119. https://doi.org/10.1016/j.virol.2006.09.036.
39. Blay WM, Kasprzyk T, Misher L, Richardson BA, Haigwood NL. 2007. Mutations in envelope gp120 can impact proteolytic processing of the gp160 precursor and thereby affect neutralization sensitivity of human immunodeficiency virus type 1 pseudoviruses. J Virol 81:13037–13049. https://doi.org/10.1128/JVI.01215-07.
40. Herrera C, Klasse PJ, Kibler CW, Michael E, Moore JP, Beddows S. 2006. Dominant-negative effect of hetero-oligomerization on the function of the human immunodeficiency virus type 1 envelope glycoprotein complex. Virology 351:121–132. https://doi.org/10.1016/j.virol.2006.03.003.
41. Leaman DP, Kinkead H, Zwick MB. 2010. In-solution virus capture assay helps deconstruct heterogeneous antibody recognition of human immunodeficiency virus type 1. J Virol 84:3382–3395. https://doi.org/10.1128/JVI.02363-09.
42. Tong T, Crooks ET, Osawa K, Binley JM. 2012. HIV-1 virus-like particles bearing pure env trimers expose neutralizing epitopes but occlude nonneutralizing epitopes. J Virol 86:3574–3587. https://doi.org/10.1128/JVI.06938-11.
43. Moore PL, Crooks ET, Porter L, Zhu P, Cayanan CS, Grise H, Corcoran P, Zwick MB, Franti M, Morris L, Roux KH, Burton DR, Binley JM. 2006. Nature of nonfunctional envelope proteins on the surface of human immunodeficiency virus type 1. J Virol 80:2515–2528. https://doi.org/10.1128/JVI.80.5.2515-2528.2006.
44. McKeating JA, McKnight A, Moore JP. 1991. Differential loss of envelope glycoprotein gp120 from virions of human immunodeficiency virus type 1 isolates: effects on infectivity and neutralization. J Virol 65:852–860.
45. Hammonds J, Chen X, Ding L, Fouts T, De Vico A, zur Megede J, Barnett S, Spearman P. 2003. Gp120 stability on HIV-1 virions and Gag-Env pseudovirions is enhanced by an uncleaved Gag core. Virology 314:636–649. https://doi.org/10.1016/S0042-6822(03)00467-7.
46. Gonzalez-Perez MP, Peters PJ, O'Connell O, Silva N, Harbison C, Cummings Macri S, Kaliyaperumal S, Luzuriaga K, Clapham PR. 2 August 2017. Identification of emerging mac-tropic HIV-1 R5 variants in brain tissue of

patients without severe neurological complications. J Virol https://doi.org/10.1128/JVI.00755-17.
47. Coutu M, Finzi A. 2015. HIV-1 gp120 dimers decrease the overall affinity of gp120 preparations for CD4-induced ligands. J Virol Methods 215-216:37–44.
48. Lu S, Manning S, Arthos J. 2000. Antigen engineering in DNA immunization. Methods Mol Med 29:355–374.
49. Wei X, Decker JM, Liu H, Zhang Z, Arani RB, Kilby JM, Saag MS, Wu X, Shaw GM, Kappes JC. 2002. Emergence of resistant human immunodeficiency virus type 1 in patients receiving fusion inhibitor (T-20) monotherapy. Antimicrob Agents Chemother 46:1896–1905. https://doi.org/10.1128/AAC.46.6.1896-1905.2002.
50. Pear WS, Nolan GP, Scott ML, Baltimore D. 1993. Production of high-titer helper-free retroviruses by transient transfection. Proc Natl Acad Sci U S A 90:8392–8396. https://doi.org/10.1073/pnas.90.18.8392.
51. Graham FL, Smiley J, Russell WC, Nairn R. 1977. Characteristics of a human cell line transformed by DNA from human adenovirus type 5. J Gen Virol 36:59–74. https://doi.org/10.1099/0022-1317-36-1-59.
52. Kong L, Sheppard NC, Stewart-Jones GB, Robson CL, Chen H, Xu X, Krashias G, Bonomelli C, Scanlan CN, Kwong PD, Jeffs SA, Jones IM, Sattentau QJ. 2010. Expression-system-dependent modulation of HIV-1 envelope glycoprotein antigenicity and immunogenicity. J Mol Biol 403:131–147. https://doi.org/10.1016/j.jmb.2010.08.033.
53. Dorfman T, Moore MJ, Guth AC, Choe H, Farzan M. 2006. A tyrosine-sulfated peptide derived from the heavy-chain CDR3 region of an HIV-1-neutralizing antibody binds gp120 and inhibits HIV-1 infection. J Biol Chem 281:28529–28535. https://doi.org/10.1074/jbc.M602732200.
54. Moore JP. 1990. Simple methods for monitoring HIV-1 and HIV-2 gp120 binding to soluble CD4 by enzyme-linked immunosorbent assay: HIV-2 has a 25-fold lower affinity than HIV-1 for soluble CD4. AIDS 4:297–305. https://doi.org/10.1097/00002030-199004000-00003.